CI&CEQ
Chemical Industry & Chemical Engineering Quarterly

Available online at
Association of the Chemical Engineers of Serbia AChE
www.ache.org.rs/CICEQ

Chem. Ind. Chem. Eng. Q. 29 (2) 161–167 (2023) CI&CEQ

PONGAYI PONNUSAMY SELVI[1]

RAJOO BASKAR[2]

[1]Department of Chemical Engineering, Kongu Engineering College, Perundurai, Tamil Nadu, India

[2]Department of Food Technology, Kongu Engineering College, Perundurai, Tamil Nadu, India

SCIENTIFIC PAPER

UDC 502/504:546.264-31

CO_2 MITIGATION STUDIES IN PACKED ABSORPTION COLUMN USING IRON OXIDE NANOFLUID

Article Highlights

- Experiments were carried out with ferromagnetic nanofluids since the agglomeration was less
- The chemical precipitation method was employed for the synthesis of iron oxide nanoparticles
- Characterization was done by SEM, TEM, and XRD analysis

Abstract

The challenging task in our ecosystem is to reduce acidic gas emissions to some extent. Many gases are emitted from the industries like H_2S, CO, CO_2, SO_2, NO, and NO_2 as exhaust gases. Among these gases, CO_2, NO_2, and SO_2 are acidic, which results in adverse effects on humans, animals, and plants. The increase in the emission of CO_2 gases from both anthropogenic and industrial sources resulted in CO_2 mitigation studies. CO_2 absorption studies were carried out using iron oxide nanofluid with the novel structured packed absorption column. Iron oxide nanoparticles were synthesized and characterized using XRD, SEM, and TEM analysis. Ammonia is used as an absorbent along with iron oxide nanofluid of three different concentrations (0.0001 w/v%, 0.001 w/v%, and 0.0015 w/v%). It was found that the iron oxide nanofluid of 0.0015 w/v% showed an improved % CO_2 removal efficiency. This enhanced % CO_2 removal efficiency was due to the increased interfacial area of the ameliorated contact between the liquid and gas phases. In addition, the magnetic field was introduced along with the packed column, which increased CO_2 removal efficiency by 1.5%.

Keywords: absorption, CO_2 removal efficiency, interfacial area, mass transfer coefficient, nanofluid, packed column.

The enormous increase in CO_2 emission resulted in rapid climatic changes, ozone layer depletion, and global warming. The increased emission of greenhouse gases into the atmosphere resulted in variable climatic conditions that paved the way for the increased atmospheric temperature [1]. Green plants utilize CO_2 present in the atmosphere during photosynthesis for food preparation for plants. But today, due to deforestation, CO_2 has not been consumed by plants, resulting in an enormous amount in the environment. Research has found that the increase in CO_2 content raises global warming [2,3]. Global Carbon Project has found an increase in CO_2 emission to about 1.9% in 2019 and 2.7% in 2021. A special Intergovernmental Panel on Climate Change report reported that carbon emissions should fall to 50% by 2030 to keep global temperatures within 1.5 °C [4,5]. An increase in coal consumption by 7.1% in India and 4.5% in China causes the release of CO_2 into the atmosphere more than the standard limit [6,7]. Two methods can shift the trend line from an increase in CO_2 emission. One is to support emission reduction, and the other is to restrict the growth of the nations that increases the emission of CO_2 [8,9,10]. The increase in the growth of renewable and low-carbon technologies accounts for strengthening emission reduction. Recent technological development should monitor the climatic impacts and drive CO_2 emission to zero by 2050 [11].

Correspondence: P.P.Selvi, Department of Chemical Engineering, Kongu Engineering College, Perundurai, Erode-638 060, Tamil Nadu, India.
E-mail: selvi.chem@kongu.edu
Paper received: 10 May, 2021
Paper revised: 5 April, 2022
Paper accepted: 1 September, 2022

https://doi.org/10.2298/CICEQ210510023S

Most of the CO_2 emission is from power plants and chemical industries. Hence advancements should be made to the present CO_2 capture technology to reduce the emission [12,13]. One such technology is Carbon Capture Sequestration (CCS). Among them, the absorption of CO_2 by chemical solvents is technically promising and can be commercialized. Research has found that the amine solutions account for the increased carbon dioxide absorption rate. Recent literature studies prove that ammonia is a promising solvent for this purpose [14]. The major advantage of ammonia over other amine solutions is that it does not degrade easily during solvent regeneration, has low energy input, and has no corrosion problem [15]. Furthermore, the use of structured packing provides the uniform distribution of the gas and solvent flow inside the absorption column and thereby increases the % CO_2 removal [16,17]. Recently nanofluids have attracted the attention of researchers for their improved functionality. It is found that the presence of iron oxide nanofluid increases the absorption of carbon dioxide into the solvent by the mechanisms like the grazing or shuttle mechanism and Brownian movement [18].

The ammonia (NH_3) solvent was used as the absorbent for further studies. Further, the % CO_2 removal, mass transfer rate per unit volume, mass transfer coefficient, mass flux, number of transfer units (NTU), and height of transfer units (HTU) for structured packing materials were studied. The structured packing material shows a better result for CO_2 absorption than the random packing material. The column loaded with the structured packing material was investigated with 12% (v/v) NH_3 concentration. To identify the best condition, 12% (v/v) solvent concentration provides higher % CO_2 removal than the other solvent concentrations. Further, the study continued to examine the enhancement of CO_2 absorption by synthesizing and adding iron oxide nanofluids. The effect of iron oxide nanofluid concentration on the % enhancement in CO_2 absorption was also studied and reported. Further, the impact of applying a magnetic field on CO_2 absorption while employing solvent with Fe_3O_4 nanoparticles was also investigated. The introduction of nanofluids was found to have a significant impact on enhancing CO_2 absorption. Iron oxide nanofluid has a wide range of applications in many fields and has good commercial potential for absorption studies. Experiments are carried out with ferromagnetic nanofluids since the agglomeration is less with ammonia as the base fluid. Many researchers used amine solvents, but only limited work is available in the literature. The chemical precipitation method is employed for the synthesis of iron oxide nanoparticles. Characterization has been done by SEM, TEM, and XRD analysis. The mass diffusion enhancement mechanism is Brownian movement, and mass diffusion reduction mechanisms are aggregation and clustering.

MATERIALS AND METHODS

Synthesis of iron oxide

Iron oxide nanoparticles were synthesized by the chemical precipitation method. First, 4 g of hydrated ferrous sulfate and hydrated ferric chloride were dissolved in 300 ml of distilled water. When the reaction temperature (80 °C) was reached, 48 ml of alkaline solution (27% NH_4OH) was added drop by drop. After this, heating and stirring continued for another 40 minutes. The brown precipitate obtained was cooled overnight. Then the precipitate was filtered, washed with distilled water and alcohol, and dried in the oven at 100 °C. Finally, the synthesized Iron oxide nanoparticles were placed in Sonicator to increase the nanofluid's stability.

XRD analysis

The Fe3O4 nanoparticles were prepared at room temperature for XRD analysis. It shows that the nanoparticles were crystalline. Fig. 1 shows the XRD analysis report of Fe3O4 nanoparticles. The most intensive lines were observed with diffraction peaks at 2θ= 36.2 and 64.1. The graph shows that Fe3O4 was in a cubic structure. The broad peaks indicate that the particles were very fine with a crystalline structure. The size of the particle was determined using Debye Scherer's formula:

XRD analysis

At the end of fermentations, the oenological parameters of mead: pH value, volatile acidity, and dry matter content, were measured [15].

The content of ethanol and methanol in mead was determined by the GC-FID method at Clarus 680 Perkin Elmer instrument with the FID detector, Elite-Wax L 60 m column, ID 0.32, DF 0.5, absolute ethanol and methanol standards, with acetonitrile as the internal standard. The injector and detector temperature of 250 °C, a sample volume of 0.5 µL, and a temperature regime of 45 °C (2 min), 45 °C/min to 245 °C (1 min). The total duration was 7.44 min, and the flow was 3 mL/min [16].

$$D = k\lambda / \beta \cos\theta \quad (1)$$

where k = 0.89 is the shape factor, λ is the X-ray wavelength of CuKα radiation, β is the full width at half maximum of the peaks, and θ is the glancing angle. The average crystallite size is 49.9 nm.

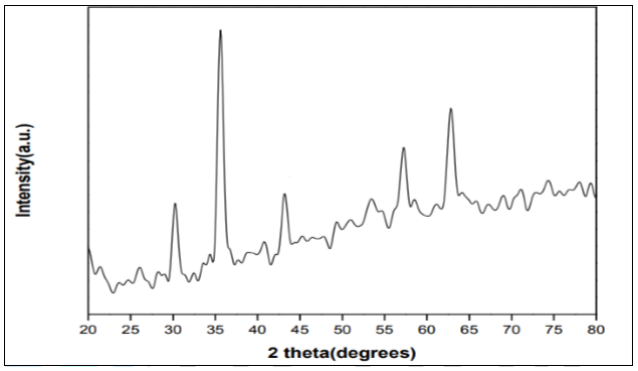

Figure 1. XRD analysis of Fe_3O_4 nanoparticles.

SEM analysis

Scanning electron microscopy (SEM) was done for the Fe_3O_4 nanoparticles, revealing the surface topography. The SEM image indicates that the particles are spherical and have well-connected grain regions. The flower-like architecture is built from several nanosheets. Fig. 2 represents the magnified SEM image of nanosheets on the spherical surface having a void.

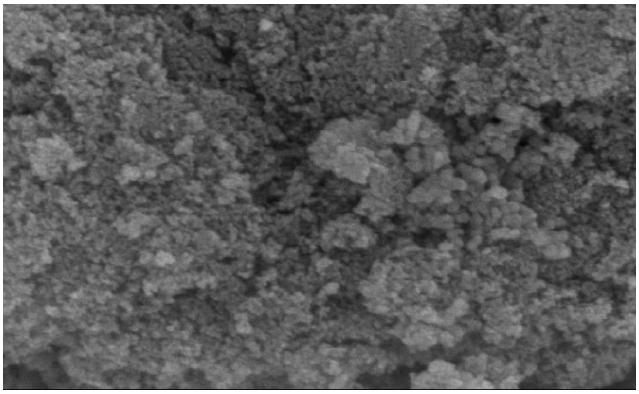

Figure 2. SEM analysis of Fe_3O_4 nanoparticles.

TEM analysis

The morphology and the size study of the synthesized Fe_3O_4 nanoparticles were done using the transmission electron microscope (TEM). The samples were prepared by dispersing the particles in de-ionized water under sonication for 30 minutes, then placing the drop onto a copper grid coated with a layer of amorphous carbon. Fig. 3 shows the TEM image of Fe_3O_4 at 50 nm magnification. The image shows that the particles were spherical when combined with the SEM image. It also shows that the particles were uniformly distributed and well connected. From this micrograph, the particles have an average diameter of 50 nm, which agrees with the result obtained by XRD.

The following equation gives the CO_2 absorption rate (NA) in the absorbent:

$$N_A = K_G P\left(y - y^*\right) \tag{2}$$

where K_G is the overall mass transfer coefficient, P is the system pressure, y is the mole fraction of the components in the gas phase, and y^* is the equilibrium mole fraction of components in the gas phase. The number of transfer units (NTU) is given by:

$$NTU = \ln\left(\frac{y_1}{y_2}\right) \tag{3}$$

where y_1 and y_2 are the outlet and inlet CO_2 concentrations.

Likewise, the height of the transfer units (HTU) is given by:

$$HTU = \frac{z}{NTU} \tag{4}$$

where z is the total height of the packed tower.

The gas partial pressure (ΔP_L) is the log mean average of inlet and outlet partial pressures. The overall mass transfer coefficient is determined by:

$$K_G\alpha = \frac{N_A}{z\ A_C\ P_T\ \Delta y} \tag{5}$$

where K_G is the mass transfer coefficient, α is the specific interfacial area in m^2/m^3, Ac is the area of the column in m^2, P_T is the total pressure in atm, and Δy is the difference in the mole fraction.

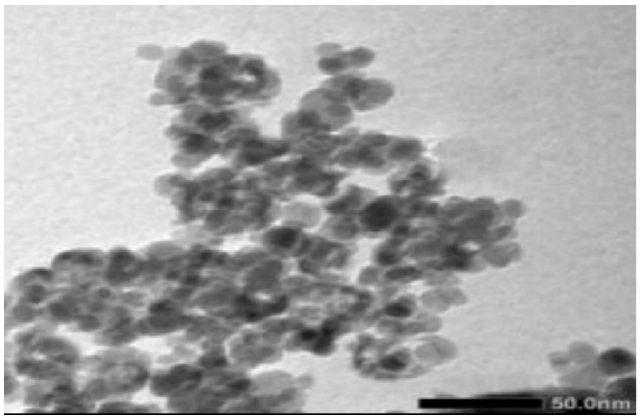

Figure 3. TEM analysis of Fe_3O_4 nanoparticles.

Experimental setup

The experimental setup for the packed absorption column is shown in Fig. 4. The packed column was made of glass with 0.6 m in height and 0.05 m inside diameter. The column was filled with a laboratory BX-DX structured packing material with an outer diameter of 0.045 m and a height of 0.05 m. The porosity of the packing material is 90%, and the specific surface area is about 250 m^2/m^3–750 m^2/m^3. Experimental conditions of the structured packed column are given in Table 1.

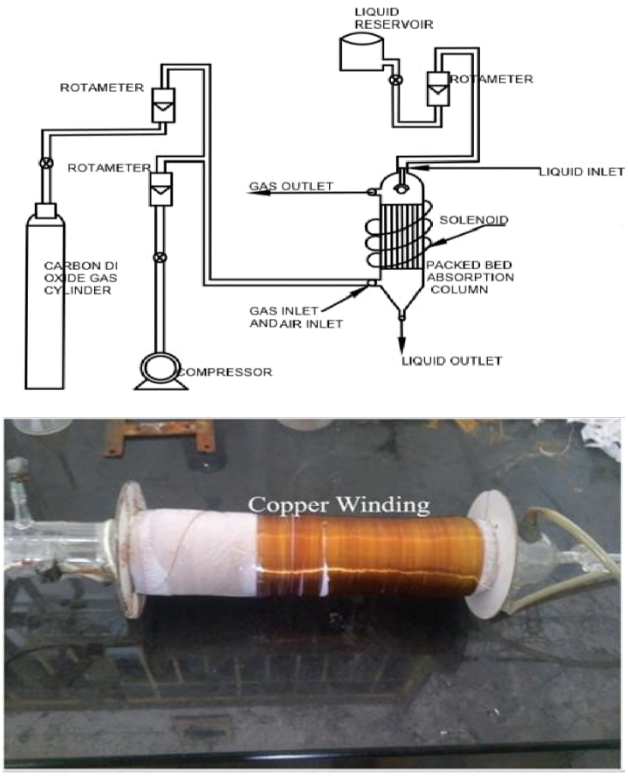

Figure 4. Schematic diagram of the experimental setup with the external magnetic field.

Table 1. Experimental conditions of the structured packed column.

No.	Parameter	Conditions
1	Absorption solvent	Aqueous NH_3 solution
2	Gas flow rate, L min^{-1}	9, 12, 14, 17, 19, 21, 23
3	CO_2: Air ratio	4:1
4	Liquid flow rate, L h^{-1}	
5	NH_3 conc. % (v/v)	2, 4, 6, 8, 10, 12
6	Temperature, °C	28

Both the gas and solvent flow rates were controlled by the flow meters. The CO_2 gas and the compressed air were passed through the packed column from its bottom. When the mixture gas reached a steady state, the aqueous ammonia solution was pumped into the column from its top. After that, the reacted sample was collected in the reservoir. The collected reacted sample was titrated against 0.1N HCl because ammonium carbonate was formed during the reaction of the gas mixture, which was a weak base and should be titrated against strong acid. The iron oxide nanoparticles were taken at 0.0001% (w/v), 0.001% (w/v), and 0.0015% (w/v). For stability of nanoparticles in the base liquid, it was kept in the ultra sonicator for 3 h. The prepared nanoparticle was immediately sent to the container and used in the CO_2 capture to prevent the deposition of the nanoparticles [19,20].

A coil of 1.1 mm thick copper wire with windings was wrapped around the external surface of the absorption column to generate a homogeneous magnetic field. The height of the coil was 0.5 m, placed in the middle part of the column, and a maximum electrical current of 2 A was applied to the coil.

RESULTS AND DISCUSSION

CO_2 absorption with structured packing employing iron oxide nano fluid with solvent

Iron oxide nanoparticles were dissolved in the 12% (v/v) ammonia solvent at concentrations ranging from 0.0001% (w/v) to 0.0015% (w/v). A significant increase in CO_2 absorption was seen at 0.0001% (w/v), 0.001% (w/v), and 0.0015% (w/v). Among them, 0.0015% (w/v) at 12% (v/v) ammonia shows better results. The removal efficiency was increased to 98%, which was previously 74% at 12% (v/v) ammonia without nanofluids. It was also found that there was a significant increase in the absorption rate, NTU, and mass transfer coefficient when iron oxide nanofluids were introduced. Compared to graphene oxide nanoparticles, iron oxide-based nanofluids show 5% better CO_2 absorption because the size of the iron oxide nanoparticles was 50 nm, much less than 100 nm graphene oxide nanoparticles. Hence the agglomeration of the particles was less in iron oxide than in graphene oxide nanoparticles. Also, the surface area created for the adsorption of CO_2 into nanoparticles was larger in the case of iron oxide nanoparticles. Similar results have been reported by [21] with different nanofluids in a packed column.

Brownian movement and micro-convection of a particle is an effect of the thermal motion of the molecular agitation of the liquid medium. Much stronger random displacement of a particle is usually observed in a less viscous liquid, with smaller particle size and higher temperature. The velocity field in the fluid, created by the Brownian motion of nanoparticles, can be responsible for such enhancement.

Effect of solvent flow rate on % CO_2 removal

The effect of solvent flow rate on CO_2 removal for the structured packing material with 12% (v/v) solvent concentration for the different iron oxide nanofluid concentrations, varying from 0.0001% (w/v) to 0.0015% (w/v), was shown in Fig. 5. It was observed that for 0.0001% (w/v) of Fe_3O_4 nanofluid the percentage of CO_2 removal was 78%, and for 0.001% (w/v) of Fe_3O_4 nanofluid, the percentage of CO_2 removal is almost 83%. At the higher concentration of Fe_3O_4 nanofluids, the percentage of CO_2 removal is 98%. It may be due to the increase in the concentration of nanoparticles

resulting in increased surface area for CO_2 absorption. CO_2 removal without nanofluids is 74%. Similar results have been reported in the previous study [21] in the packed column with nanofluids.

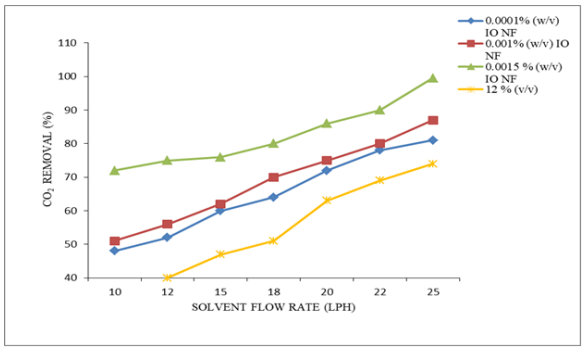

Figure 5. Effect of solvent flow rate on % CO_2 removal by employing iron oxide nanofluid and magnetic field.

Effect of solvent flow rate on rate of absorption

The effect of solvent flow rate on the absorption rate for the structured packing material with a 12% (v/v) solvent concentration for different iron oxide nanofluid concentrations (varying from 0.0001% (w/v) to 0.0015% (w/v) is shown in Fig. 6. The rate of CO_2 absorption was 0.0023 kmol/m^3s for 0.0001% (w/v) and for 0.001% (w/v) and 0.0015% (w/v) Fe_3O_4 nanofluids the rate of CO_2 absorption was 0.0025 kmol/m^3s. The mass transfer rate was enhanced with nanoparticles in a gas-liquid system. It was a gas transfer phenomenon from the gas-liquid phase to the liquid phase by gas adsorption in the dispersed Fe_3O_4 nanoparticles. Hence, the gas concentration near the interface will decrease, resulting in absorption enhancement. Similar results were reported in the previous study by [21] in the packed column with nanofluids.

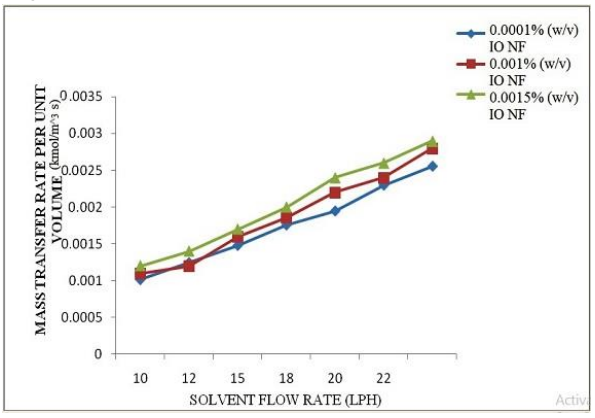

Figure 6. Effect of solvent flow rate on the rate of absorption by employing iron oxide nanofluid and magnetic field.

Effect of solvent flow rate on the number of transfer units

The effect of solvent flow rate on NTU for structured packing material with a 12% (v/v) solvent concentration for different iron oxide nanofluid concentrations (varying from 0.0001% (w/v) to 0.0015% (w/v) was shown in Fig. 7. The NTU value increases for a low Fe_3O_4 nanofluid concentration of 0.0001% (w/v) than 0.001% (w/v) and 0.0015% (w/v) due to the better magnetic iron particles that produce thermal energy leading to a low NTU value. Similar results have been reported in the previous study [22] in the packed column with nanofluids.

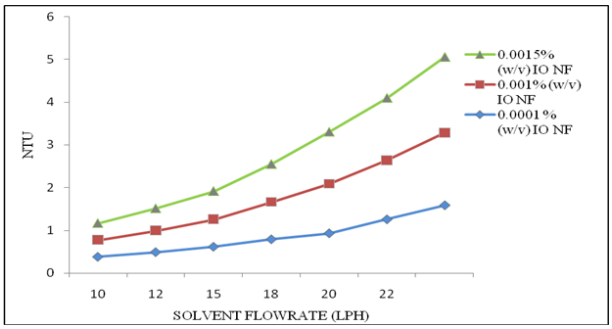

Figure 7. Effect of solvent flow rate on NTU by employing iron oxide nanofluid and magnetic field.

Effect of solvent flow rate on height of transfer unit

The effect of solvent flow rate on HTU for the structured packing material with a 12% (v/v) solvent concentration for the different iron oxide nanofluid concentrations (varying from 0.0001% (w/v) to 0.0015% (w/v) was shown in Fig. 8. The height of transfer unit is almost 1.6 for 0.0001% (w/v) iron oxide nanofluids. For higher nanofluids of 0.001% (w/v) and 0.0015% (w/v), the HTU value is 0.8. It was further observed that a lower value of HTU results in a high absorption performance. Similar results have been reported in a previous study [22] in the packed column with nanofluids.

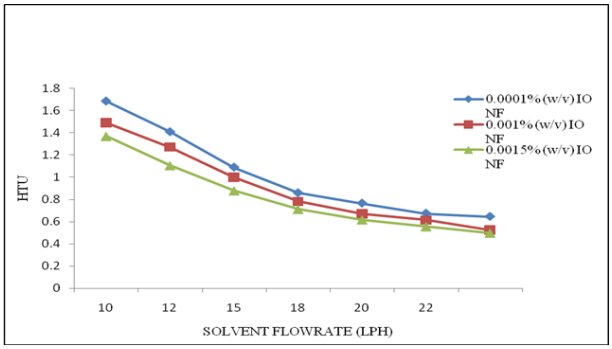

Figure 8. Effect of solvent flow rate on HTU by employing iron oxide nanofluid and magnetic field.

Effect of solvent flow rate on volumetric overall mass transfer coefficient

The effect of the solvent flow rate on the mass transfer coefficient for the structured packing material with a 12% (v/v) solvent concentration for different iron oxide nanofluid concentrations (varying from 0.0001% (w/v) to 0.0015% (w/v) is shown in Fig. 9. The mass

transfer coefficient increases with an increase in the solvent flow rate for all three Fe_3O_4 nanofluid concentrations. But for 0.0015% (w/v), iron oxide nanofluids increase the volumetric overall mass transfer coefficient to 27 kmol/h m^3. This increase in the overall volumetric mass transfer coefficient was due to the addition of magnetic iron oxide nanofluids in the absorbent. Similar results have been reported in the previous study by [23] in the packed column with nanofluids.

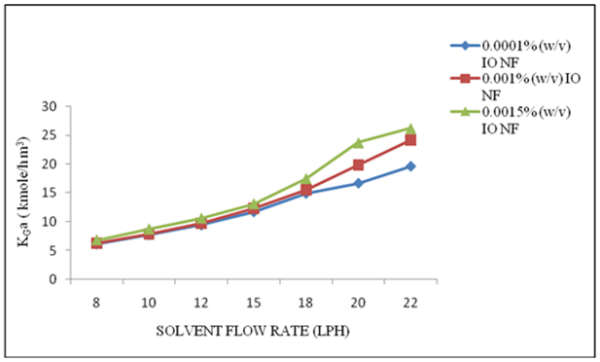

Figure 9. Effect of solvent flow rate on volumetric overall mass transfer coefficient by employing iron oxide nanofluid and magnetic field.

Optimum values of operational parameters

The efficiencies of the random and structured packing material in CO_2 removal are compared in Table 2. The structured packing material is more efficient in CO_2 removal than the random packing material. On the other hand, the efficiency of iron oxide with a magnetic field in CO_2 removal is higher than the efficiency of iron oxide, as can be seen in Table 3.

Table 2. Comparison between the random and structured packing material.

S.No.	% CO_2 removal	
	12% Random packing material	12% Structured packing material
1	30	34
2	36	40
3	44	47
4	47	51
5	57	63
6	58	69
7	62	74

Table 3. Comparison of % CO_2 removal for iron oxide and iron oxide with a magnetic field.

S.No.	Iron Oxide	Iron Oxide+ Magnetic Field
1	70	73
2	76	79
3	80	84
4	85	88
5	89	91
6	92	94
7	98	99.5

CONCLUSION

The CO_2 gas absorption studies were carried out in a packed absorption column. The selection of suitable solvent, comparison of random and structured packing material performance, enhancement of absorption by adding iron oxide nanoparticles in a solvent, and induction of magnetic field were in detail studied. As a result, the following conclusions were drawn.

Among the different solvents considered, NH_3 was the best for CO_2 gas absorption. Furthermore, structured packing resulted in higher efficiency than random packing. The CO_2 removal increased with an increase in the NH_3 concentration, and about 74% CO_2 removal was achieved. With the introduction of nanofluid like Fe_3O_4 along with the absorbent, the % CO_2 removal increased by 98%. Moreover, the Fe_3O_4 nanofluid showed a better result than the other nanofluids under all conditions because the other nano fluid settled in the solvent, whereas Fe_3O_4 was a magnetite form with better paramagnetic properties and lesser particles agglomerated. The paramagnetic nature of Fe_3O_4 particles favored the further marginal enhancement of CO_2 removal up to 99.5% with the application of an external magnetic field, whereas a 12% enhancement was seen [9]. The captured CO_2 from the packed column can be used in the product synthesis. The absorption kinetics of CO_2 over a while could be studied. CO_2 sequestration can be tried with hybrid nanofluids and also by varying particle size. The applied electric current to induce a magnetic field in this study is 2 mA, and future studies can be conducted by varying the electric current. Similarly, NO_2, and SO_2 sequestrations can also be examined in the structured packed column with nanofluids and the magnetic field.

REFERENCES

[1] A. Aroonwilas, Ind. Eng. Chem. Res. 43 (2004) 2228–2237. https://doi.org/10.1021/ie0306067.

[2] A. Aroonwilas, P. Tontiwachwuthikul, Chem. Eng. Sci. 55 (2000) 3651–3663. https://doi.org/10.1016/S0009-2509(00)00035-X.

[3] W.M.Budzianowski, R.Miller, Recent Pat. Mech. Eng. 2 (2009) 228–239. https://doi.org/10.2174/1874477X10902030228.

[4] T.W. Chien, H. Chu, H.T. Hsueh, J. Environ. Eng. 129 (2003) 967–974. https://doi.org/10.1061/(ASCE)0733-9372(2003)129:11(967).

[5] F. Zhang, C.-G. Fang, Y.-T. Wu, Y.-T. Wang, A.-M. Li, Z.-B. Zhang, Chem. Eng. J. 160 (2010) 691–697. https://doi.org/10.1016/j.cej.2010.04.013.

[6] H. Monnier, L. Falk, Chem. Eng. Sci. 66 (2011) 2475–2490. https://doi.org/10.1016/j.ces.2011.01.016.

[7] H. Monnier, L. Falk, N. Mhiri, Chem. Eng. Process. 49 (2010) 953–957. https://doi.org/10.1016/j.cep.2010.05.001.

[8] J. Salimi, F. Salimi, Rev. Mex. Ing. Quim. 15 (2016) 185–192. http://www.rmiq.org/ojs311/index.php/rmiq/article/view/1106/413.

[9] J. Salimi, F. Salimi, Heat Mass Transfer 51 (2015) 621–629. https://doi.org/10.1007/s00231-014-1439-5.

[10] A.O. Lawal, R.O. Idem, Ind. Eng. Chem. Res. 45 (2006) 2601–2607. https://doi.org//10.1021/ie050560c.

[11] R. Notz, N. Asprion, I. Clausen, H. Hasse, Chem. Eng. Res. Des. 85 (2007) 510–515. https://doi.org/10.1205/cherd06085.

[12] P. Oinas, G. Wild, N. Midoux, H. Haario, Chem. Eng. Process. 34 (1995) 503–513. https://doi.org/10.1016/0255-2701(95)00454-8.

[13] O. Lawal, A. Bello, R. Idem, Ind. Eng. Chem. Res. 44 (2005) 1874–1879. https://doi.org/10.1021/ie049261y.

[14] Z. Niu, Y. Guo, Q. Zeng, W. Lin, Ind. Eng. Chem. Res. 51 (2012) 5309–5319. https://doi.org/10.1021/ie2030536.

[15] Q. Zeng, W. Lin, Y. Guo, Z. Niu, Fuel Process. Technol. 108 (2013) 76–81. https://doi.org/10.1016/j.fuproc.2012.05.005.

[16] P.P. Selvi, R. Baskar, P.S. Nair, J. Adv. Chem. 13 (2017) 6520–6523. https://doi.org/10.24297/jac.v13i10.5789.

[17] P.P. Selvi, R. Baskar, J. Chem. Soc. Pak. 41 (2019) 820–824. https://jcsp.org.pk/PublishedVersion/3b17aa02-80a4-466d- aaa9- cff35adc7448Manuscript%20no%2010,%20Final%20Gally%20Proof%20of%2011943%20(Pongayi%20Ponnusamy%20Selvi).pdf.

[18] P.P. Selvi, R. Baskar, Chem. Ind. Chem. Eng. Q. 26 (2020) 321–328. https://doi.org/10.2298/CICEQ181225008S.

[19] S.-S. Ashrafmansouri, M.N. Esfahany, Inter. J. Therm. Sci. 82 (2014) 84–99. https://doi.org/10.1016/j.ijthermalsci.2014.03.017.

[20] W. Yu, H. Xie, J. Nano Mater. 2012 (2011) ID 435873. https://doi.org/10.1155/2012/435873.

[21] W. Hao, E. Bjorkman, M. Lilliestrale, N. Hedin, Chem. Sustainability 7 (2014) 875–882. https://doi.org/10.1002/cssc.201300912.

[22] W. Yuan, B. Li B, L. Li, Appl. Surf. Sci.257 (2011) 10183–10187. https://doi.org/10.1016/j.apsusc.2011.07.015.

[23] Z. Zhang, W. Zhang, X. Chen, Q. Xia, Z. Li, Sep. Sci. Technol. 45 (2010) 710–719. https://doi.org/10.1080/01496390903571192.

[24] M. M. Tun, D. Juchelková, Environ. Eng. Res. 24 (2019) 618–629. http://dx.doi.org/10.4491/eer.2018.327.

[25] Z. Samadi, M Haghshenasfard, A Moheb, Chem. Eng. Technol. 37 (2014) 462–470. https://doi.org/10.1002/ceat.201300339.

[26] M. Ansaripour, M Haghshenasfard, A Moheb, Chem. Eng. Technol. 41 (2018) 367–378. https://doi.org/10.1002/ceat.201700182.

[27] M.Khani, M. Haghshenasfard, N. Etesami, M.R. Talaei, J. Mol. Liq. 334 (2021) 116078. https://doi.org/10.1016/j.molliq.2021.116078.

PONGAYI PONNUSAMY SELVI[1]

RAJOO BASKAR[2]

[1]Department of Chemical Engineering, Kongu Engineering College, Perundurai, Tamil Nadu, India

[2]Department of Food Technology, Kongu Engineering College, Perundurai, Tamil Nadu, India

NAUČNI RAD

ISTRAŽIVANJA UKLANJANJA CO_2 U APSORPCIONOJ KOLONI SA PAKOVANJEM KORIŠĆENJEM NANOFLUIDA SA OKSIDOM GVOŽĐA

Izazovan zadatak u našem ekosistemu je da u određenoj meri smanjimo emisije kiselih gasova. Mnogi gasovi se emituju iz industrija, kao što su H_2S, CO, CO_2, SO_2, NO i NO_2. Među ovim gasovima, CO_2, NO_2 i SO_2 su kiseli, što dovodi do štetnih efekata na ljude, životinje i biljke. Povećanje emisije CO_2 gasova iz antropogenih i industrijskih izvora iniciralo je studije uklanjanja CO_2. Studije apsorpcije CO_2 su sprovedene korišćenjem nanofluida sa gvožđe-oksidom sa novom apsorpcionom kolonom sa strukturiranim pakovanjem. Nanočestice oksida gvožđa su sintetizovane i okarakterisane KSRD, SEM i TEM analizom. Amonijak se koristi kao apsorbent zajedno sa nanofluidom sa oksidom gvožđa u tri različite koncentracije (0,0001%, 0,001% i 0,0015%). Utvrđeno je da je ovaj nanofluid u koncentraciji od 0,0015% pokazao poboljšanu efikasnost uklanjanja CO_2. Ova poboljšana efikasnost uklanjanja % CO_2 je rezultat povećane međufazne površine poboljšanog kontakta između tečne i gasne faze. Pored toga, magnetno polje je razvijeno duž kolone, što je povećalo efikasnost uklanjanja CO_2 za 1,5%.

Ključne reči: apsorpcija, efikasnost uklanjanja CO_2, međufazna površina, koeficijent prenosa mase, nanofluid, kolona sa pakovanjem.